



IAEA

International Atomic Energy Agency

INDC(AUS)-0020
Distr. G+J

INDC International Nuclear Data Committee

Cross sections of n-³He between 3.5 and 30 MeV. An evaluation using results of an ab-initio calculation

M. Drosig

Faculty of Physics, Univ. Vienna, Vienna, Austria

and

A. Deltuva

Institute of Theoretical Physics and Astronomy, Vilnius University, Vilnius, Lithuania

October 2016

Selected INDC documents may be downloaded in electronic form from

<http://www-nds.iaea.org/publications/>

or sent as an e-mail attachment.

Requests for hardcopy or e-mail transmittal should be directed to

nds.contact-point@iaea.org

or to:

Nuclear Data Section
International Atomic Energy Agency
Vienna International Centre
PO Box 100
A-1400 Vienna
Austria

Produced by the IAEA in Austria
October 2016

Cross sections of n-3He between 3.5 and 30 MeV. An evaluation using results of an ab-initio calculation

M. Drogg

Faculty of Physics, Univ. Vienna, Vienna, Austria

and

A. Deltuva

Institute of Theoretical Physics and Astronomy, Vilnius University, Vilnius, Lithuania

Abstract

The availability of cross section predictions from an ab-initio calculation of the n-3He system in the energy range from 3.5 to 30 MeV neutron energy allows improvement of the neutron cross section evaluation in this energy range. In agreement with the most recent evaluation, this calculation corroborates the lower solution for the total cross data values. New insight in the differential elastic cross sections is obtained, on the one hand a 3.7% increase of the scale is suggested, on the other hand excitation functions are verified over the wide energy range under consideration. Experimental evidence backing this 3.7% increase of the elastic cross sections is presented. Consequently, revised values for the total, elastic, and break-up cross sections are presented. Experimental differential elastic cross sections must be up-scaled whereas the two-body nonelastic differential cross sections remain unchanged.

October 2016

Table of Contents

I. INTRODUCTION	7
II. CROSS SECTION COMPARISONS	8
A. TOTAL CROSS SECTIONS	8
B. CROSS SECTIONS OF THE TWO NONELASTIC TWO-BODY REACTIONS	9
III. REEVALUATIONS.....	19
IV. DISCUSSION.....	23
REFERENCES.....	25

Cross sections of n-³He between 3.5 and 30 MeV. An evaluation using results of an ab-initio calculation

M. Drogg,^{*} and A. Deltuva[†]

^{*}Faculty of Physics, University of Vienna, Boltzmannngasse 5, A-1090, Vienna, Austria

[†] Institute of Theoretical Physics and Astronomy, Vilnius University, Saulėtekio al. 3, LT-10222 Vilnius, Lithuania

ABSTRACT

The availability of cross section predictions from an ab-initio calculation of the n-³He system in the energy range from 3.5 to 30 MeV neutron energy allows improvement of the neutron cross section evaluation in this energy range. In agreement with the most recent evaluation, this calculation corroborates the lower solution for the total cross section values. New insight in the differential elastic cross sections is obtained, on the one hand a 3.7% increase of the scale is suggested, on the other hand excitation functions are verified over the wide energy range under consideration. Experimental evidence backing this 3.7% increase of the elastic cross sections is presented. Consequently, revised values for the total, elastic, and break-up cross sections are presented. Experimental differential elastic cross sections must be up-scaled whereas the two-body nonelastic differential cross sections remain unchanged.

I. INTRODUCTION

A comparison of ab-initio calculated cross sections¹ with the latest evaluated experimental cross sections²⁻⁴ may not only give insight in the quality of the ab-initio calculation but may result in improved evaluated data. For the first purpose experimental data with the highest confidence must be used whereas those with less confidence may profit from the inclusion of the calculated values in data analysis. As the numerical accuracy in solving exact four-nucleon equations is well under control¹ the ability of realistic nucleon-nucleon force models to predict data is under scrutiny.

The most accurate neutron cross sections are the total ones with typical uncertainties <1%. Then there are neutron cross sections measured via associated charged particles with uncertainties as low as 1.5%. Neutron cross sections measured relative to a neutron cross section standard, e.g., the elastic n-¹H scattering, will have uncertainties in excess of 2.5%.

Thus, the first two qualify for checking the ab-initio calculation whereas the third type of cross sections may profit from the calculated predictions.

II. CROSS SECTION COMPARISONS

A. TOTAL CROSS SECTIONS

TABLE I gives three data sets describing the energy dependence of the n-³He total cross section between 3.5 and 30 MeV. The difference between the calculated data and the two competing experimental data sets^{5,6} is illustrated in Fig. 1.

TABLE I. Calculated total cross sections compared to the evaluated, and the Karlsruhe data.

E_n (MeV)	Xsect. ^{a)} barns	Xsect. ^{b)} barns	Xsect. ^{c)} barns
3.5	2.654	2.760	2.876
5.0	2.295	2.378	2.458
5.5	2.179	2.254	2.332
6.0	2.085	2.139	2.215
7.0	1.902	1.937	2.011
8.0	1.745	1.763	1.837
10.0	1.493	1.513	1.561
12.0	1.302	1.317	1.360
14.4	1.125	1.130	1.170
16.0	1.029	1.039	1.078
17.1	0.9739	0.986	1.021
22.0	0.7801	0.791	0.815
23.7	0.7258	0.738	0.765
27.0	0.6450	0.6522	0.673
30.0	0.5846	0.5898	0.609

^{a)}calculated values from Ref. 1

^{b)}measured values from Ref. 5 as used in the evaluations^{2,4}

^{c)}measured values from Ref. 6, “Karlsruhe data”

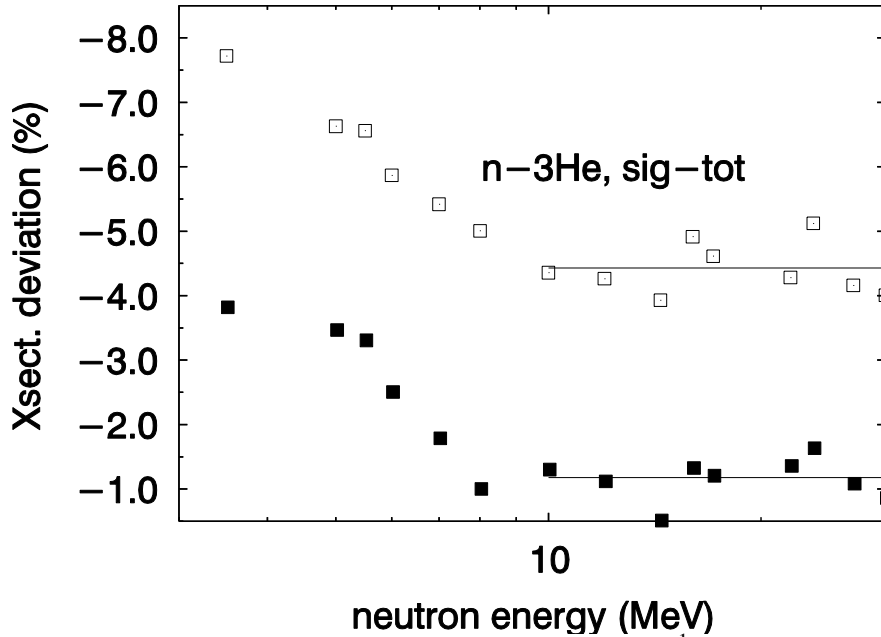


Fig. 1. Percent deviations of the calculated total cross sections¹ from the data of Goulding et al.⁵ (full rectangles) and from the Karlsruhe data⁶ (open rectangles). The horizontal lines show the average values of the data above 10 MeV.

The excellent agreement of the energy dependence between about 8 (near 7.337 MeV, the threshold energy of the reaction ${}^3\text{He}(n,np){}^2\text{H}$) and 30 MeV indicates that the calculation, in essence, works correctly. Whereas the data of Goulding⁵ et al. are 1.2% higher, i.e., deviating about one standard deviation of these data, the Karlsruhe data⁶ are higher by 4.4%, i.e., off by about four standard deviations. Such a difference between these two data sets of 2.35% was reported before². This supports the finding of the evaluation^{2,4} that only the data of Goulding et al.⁵ are consistent with the bulk of the other experimental data. Thus, these data are assumed to be correct.

B. CROSS SECTIONS OF THE TWO NONELASTIC TWO-BODY REACTIONS

There are two nonelastic two-body reactions, namely the exothermic reaction ${}^3\text{He}(n,p){}^3\text{H}$ with a Q-value of 0.7638 MeV, and the endothermic reaction ${}^3\text{He}(n,d){}^2\text{H}$ with a threshold of 4.3644 MeV. The evaluated (differential) cross sections were obtained by time-reversal from data depending on associated charge particle measurements^{3,4}. Their scale uncertainties were established as $\pm 1.5\%$, each.

As a one-by-one comparison would give an even worse result, Fig. 2 compares the energy dependences of the sum of this cross section pair. Above 10 MeV the calculated sums are lower by a few percent. This unsatisfactory situation does not warrant any change in the evaluated nonelastic cross sections due to the calculated values.

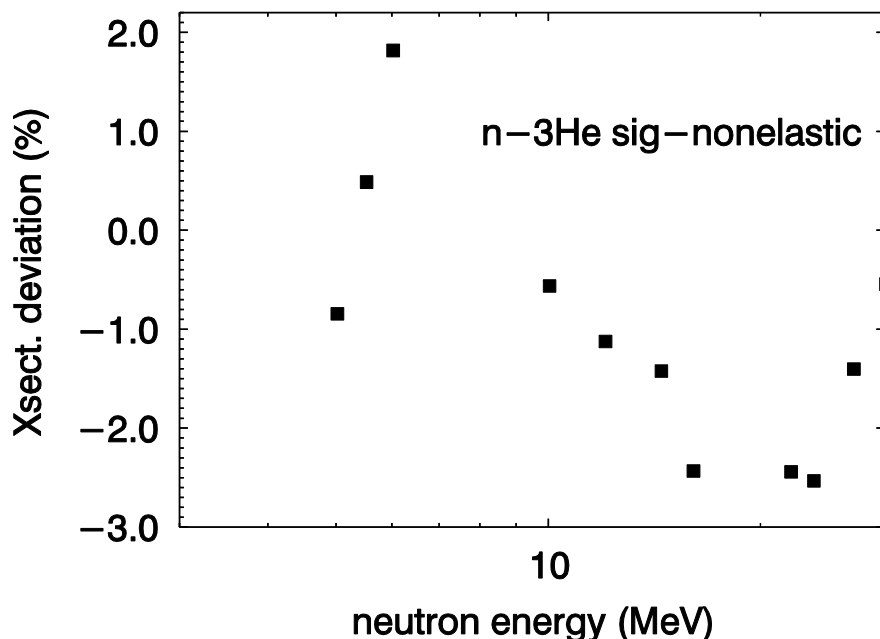


Fig. 2. Energy dependence of the percentage deviation of the calculated¹ sum of the ${}^3\text{He}(n,p){}^3\text{H}$ and the ${}^3\text{He}(n,d){}^2\text{H}$ cross sections from its evaluated^{3,4} counterpart.

C. ELASTIC (DIFFERENTIAL) CROSS SECTIONS

All elastic scattering experiments^{2,4,7-13} in the energy range of interest are listed in TABLE II. Abramov⁷ does not give cross sections and is, therefore, not considered. As detailed to much extent² the (unpublished) data of Haesner¹³ are not, as misleadingly presented in this diploma thesis, absolute angle-dependent differential cross sections but *relative* (energy-dependent) *yield* excitation functions. Thus, any comparison should be made with excitation functions to preserve the intrinsic precision of the measured data. The back angle excitation functions are of particular value, as the neutron detection efficiency at the corresponding (lower) energies of the scattered neutrons appears to be more reliable. As these data are *relative*, the information lies in the energy dependence (shape), only. The scale of the back-angle excitation functions of the (corrected) cross sections was obtained by extrapolation from 136 degrees (center-of-mass) to 180 degrees using Legendre fitting^{2,13}. Such an extrapolation is somewhat arbitrary. The present energy-independent extrapolations increase the normalization factors of the 135, 150, 160, and 178.8 degrees excitation functions by 1.047, 1.108, 1.116, and 1.140, respectively, compared to the previous ones^{2,4}. Figs. 3 through 9 compare experimental absolute angle-dependent differential cross sections at various projectile energies with their calculated predictions¹.

TABLE II. Elastic cross section measurements

Reference	Energy Range	Remarks
Abramov ⁷	1.0 to 4.5 MeV	only relative pulse height spectra
Sayres et al. ⁸	1.0, 2.7, 5.0, 8.1, and 17.5 MeV	17.5 MeV data with huge uncertainties
Antolkovic ^{9,10}	14.4 MeV	isolated 180° data point, and back angle data
Curtis ¹¹	14.1 MeV	associated charged particle data
Seagrave et al. ¹²	1.0, 2.0, 3.5, and 6.0 MeV	neutron time-of-flight, liquid scattering sample
Haesner ^{2,4,13}	5.0 to 30.0 MeV	neutron time-of-flight, liquid scattering sample
Drosg et al. ²	7.9 to 23.7 MeV	neutron time-of-flight, liquid scattering sample

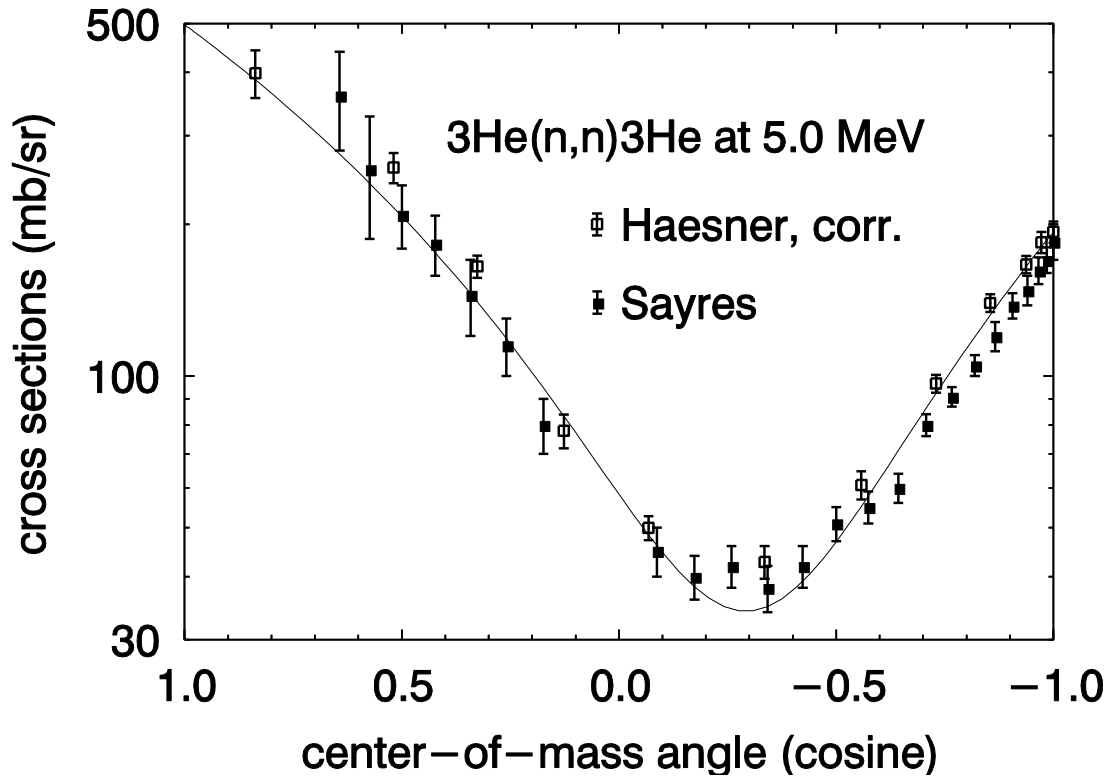


Fig. 3. Data comparison at 5.0 MeV. Experimental data of Sayres et al.⁸ and Haesner's corrected data² vs. calculated data¹ (curve)

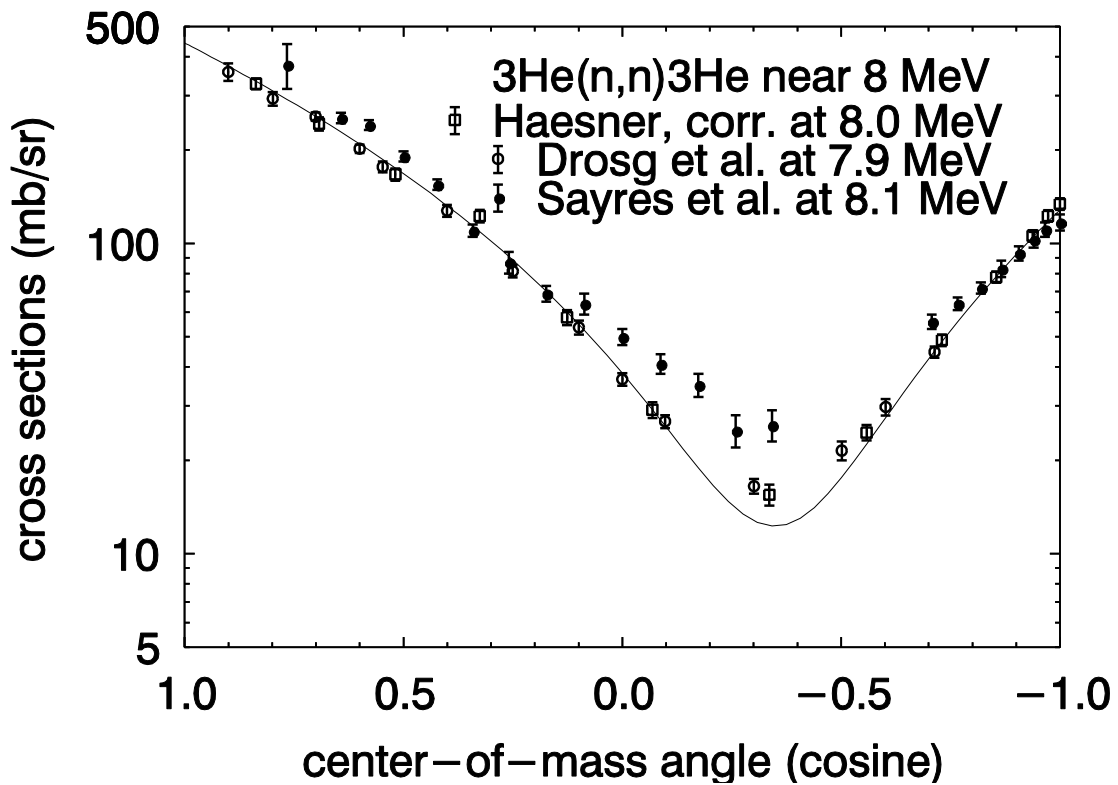


Fig. 4. Data comparison around 8 MeV. Experimental data of Sayres et al.⁸ (at 8.1 MeV), of Haesner's corrected data² (at 8.0 MeV), of Drosg et al.² (at 7.9 MeV) vs. calculated data¹ (at 8.0 MeV, curve)

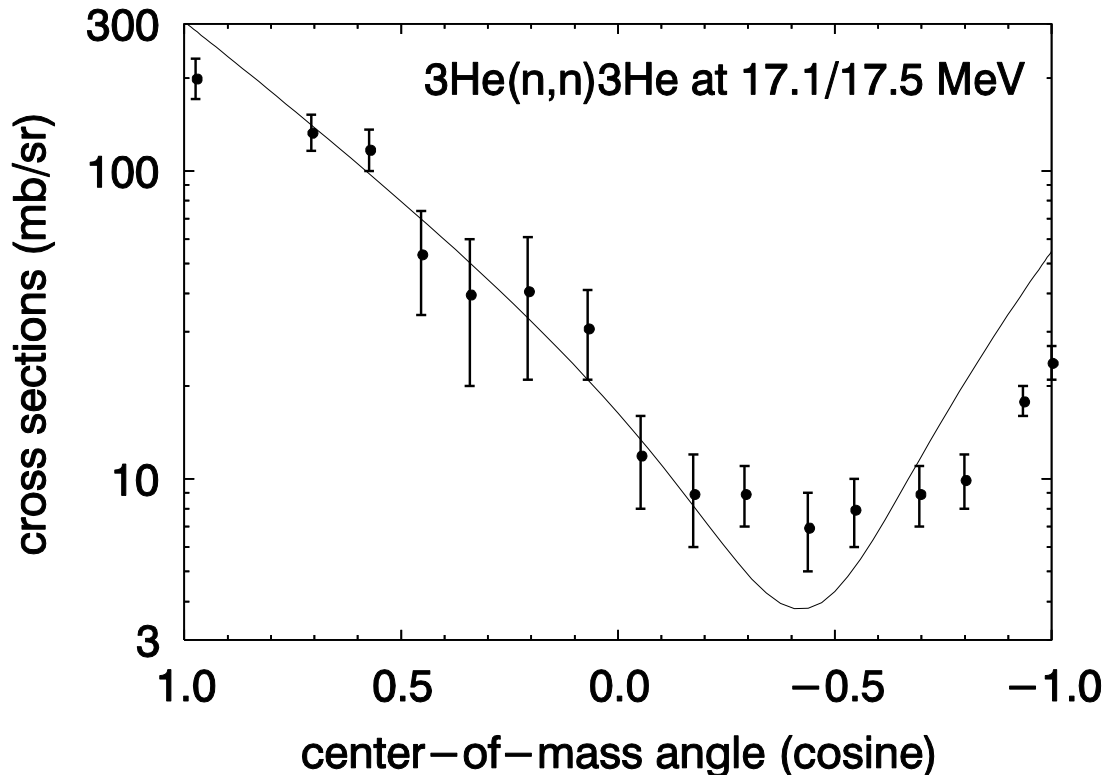


Fig. 5. Data comparison at 17.5 MeV. Experimental data of Sayres et al.⁸ vs. calculated data¹ (at 17.1 MeV, curve)

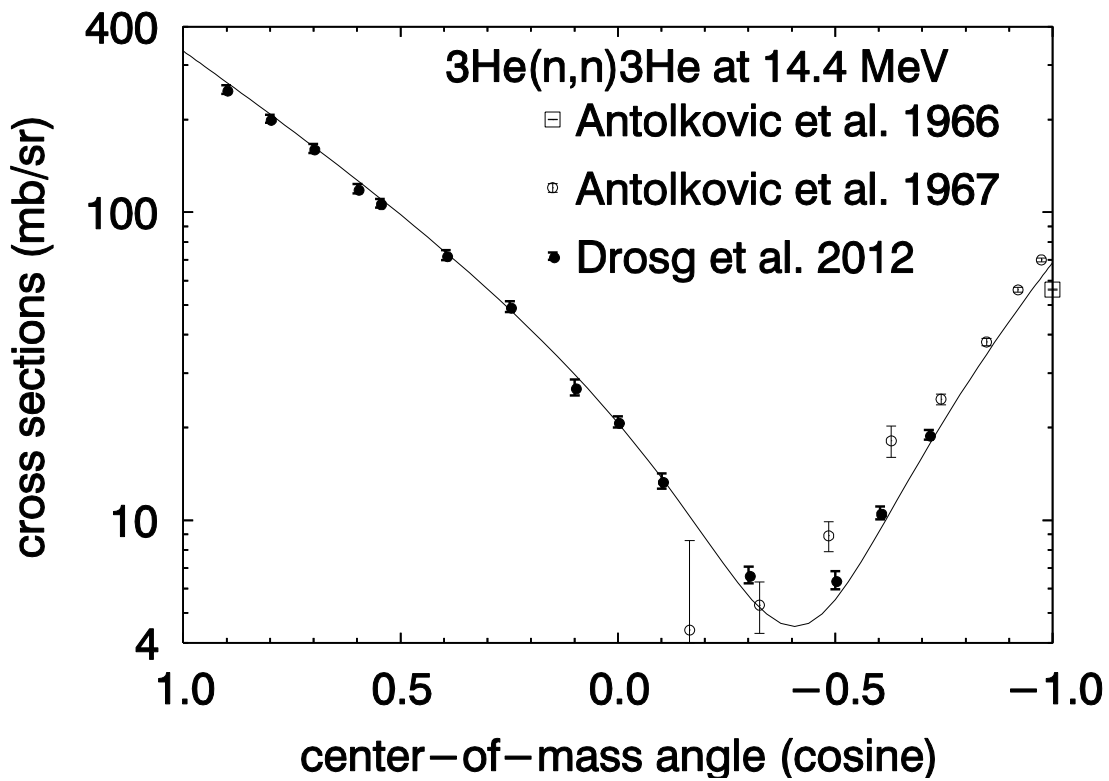


Fig. 6. Data comparison at 14.4 MeV. Experimental data sets of Antolkovic et al.^{9,10}, and Drosig et al.² vs. calculated data¹ (curve)

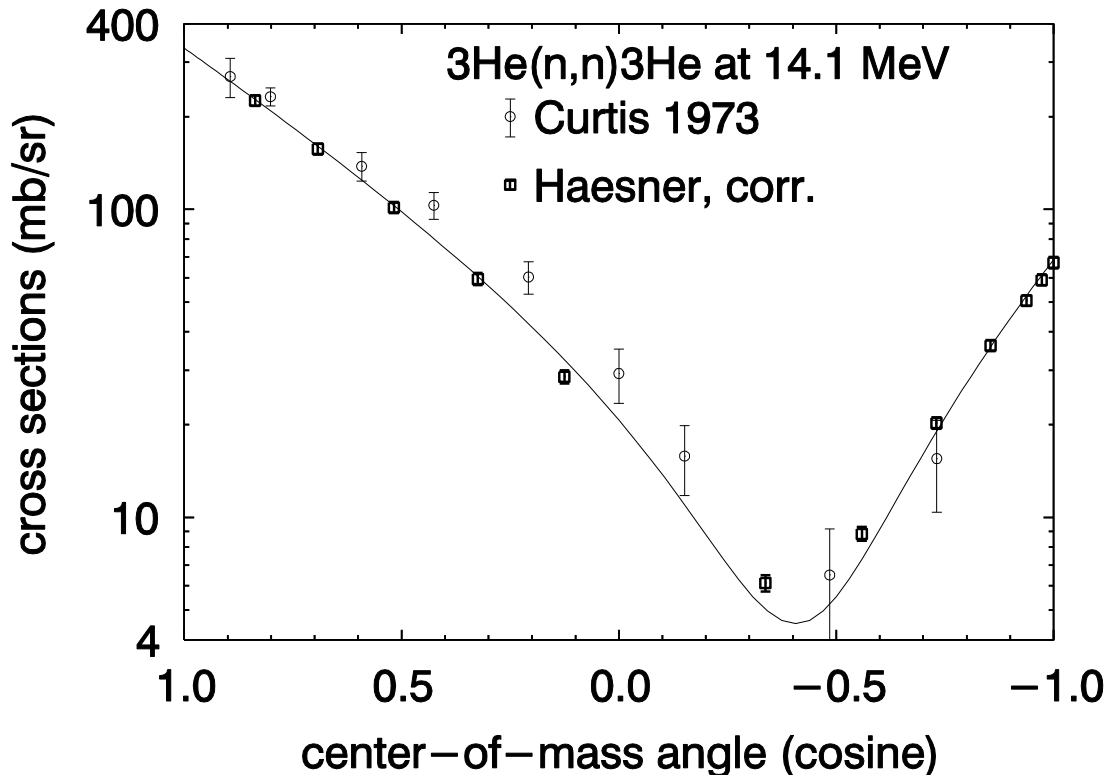


Fig. 7. Data comparison at 14.1 MeV. Experimental data of Curtis¹¹ at 14.1 MeV, and Haesner's corrected 14 MeV data² vs. calculated data¹ at 14.4 MeV (curve)

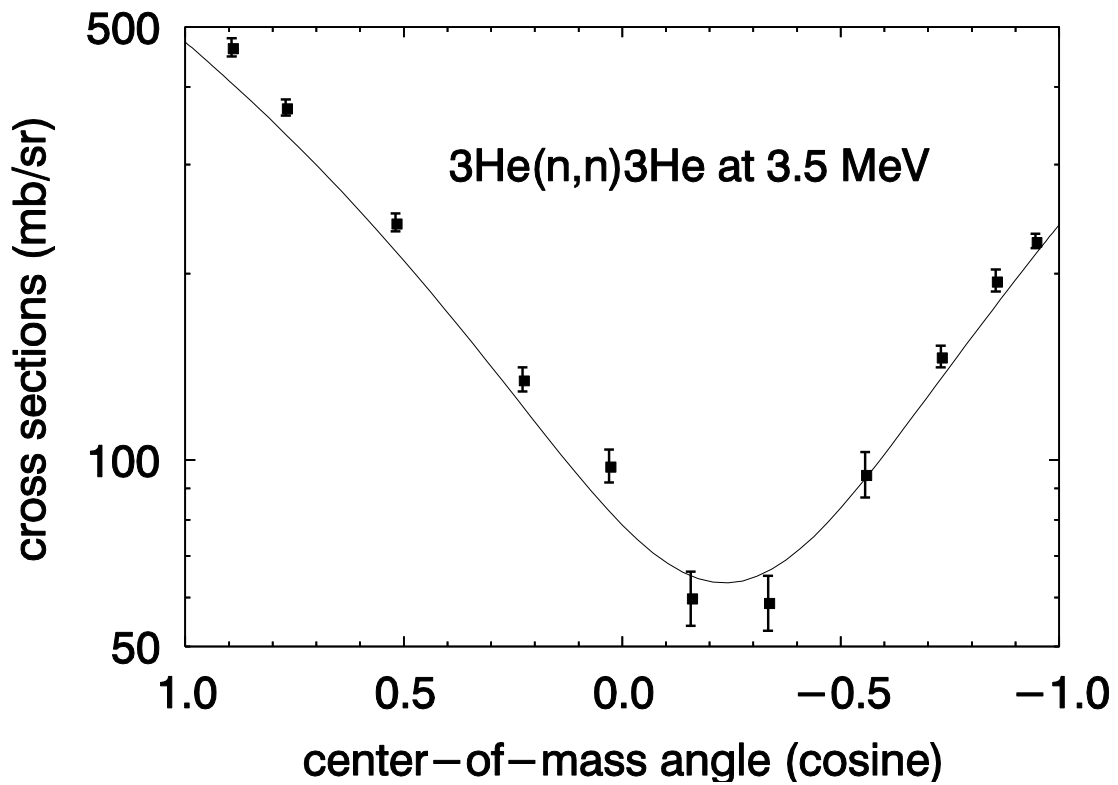


Fig. 8. Data comparison at 3.5 MeV. Experimental data of Seagrave et al.¹² vs. calculated data¹ (curve)

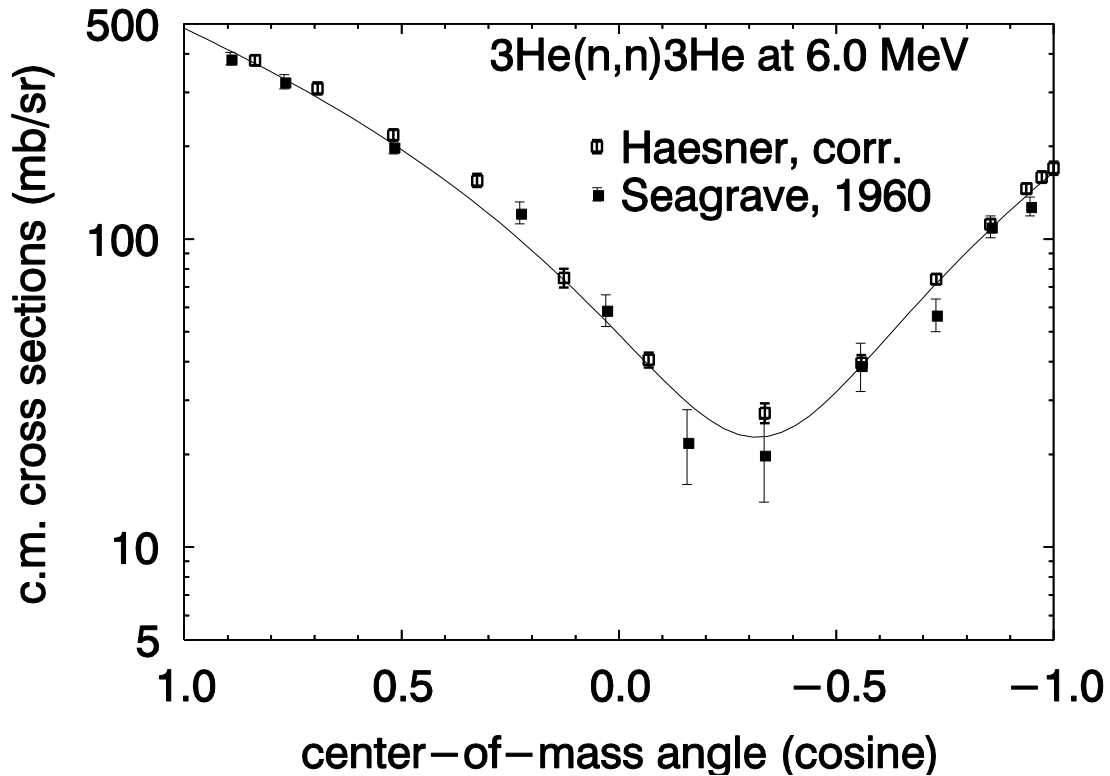


Fig. 9. Data comparison at 6.0 MeV. Experimental data of Seagrave et al.¹², and Haesner's corrected data² vs. calculated data¹ (curve)

Data comparison as done in Figs. 3 through 9 does not allow any detailed judgement on the quality of the calculation except for a general remark that “the agreement is surprisingly good”, nearly as good as that of the much simpler nucleon-deuteron system¹⁴. Thus, it is necessary to include all available information in a comparison. The data by Drogg et al.² extend to 136 degrees (c.m.) only. Their main feature is that the front portion is consistently lower by 3.7% (see TABLE III) and that the minimum is considerable flatter. The latter effect is not surprising as the uncertainty of the calculation in the minimum is on the order of 10%. A similar situation can be found in the elastic $p+{}^3\text{He}$ scattering above 20 MeV¹⁵.

TABLE III Energy dependence of the scale difference in the front portion of the angle-dependent differential cross sections (calculated¹ vs. experimental²)

E_n (MeV)	Ratio	Uncorr. scale uncertainty(%)
7.9	1.0365	2.5
12.0	1.0410	1.4
13.6	1.0382	2.5
14.4	1.0304	2.1
23.7	1.0320	2.2
average	1.0367	0.9 ^{a)} ±0.2% rms.

^{a)} 1.9% total uncertainty, when including the correlated uncertainty of 1.7%

From TABLE III the following may be concluded

- The energy dependence of the cross section ratio over this relatively wide energy range from 7.9 to 23.7 MeV is practically constant (0.2% rms. scatter!)
- Thus, an energy independent shift of the scale is suggested. This suspicion is supported by the fact that the averaged scale uncertainty of 1.9% does not account for the deviation of 3.7%. At this stage, this discrepancy cannot be fully explained.

The relative *yield* excitation functions of Haesner¹³ were later corrected and converted to absolute angle dependent differential cross sections^{2,4} using the absolute data of Drogg et al.^{2,4} to establish individual scale factors for each (corrected) excitation function. The scales of the five (relative) excitation functions between 120 and 178.8 degrees (lab.) depend on Legendre extrapolations of the data of Drogg et al.².

The main value of Haesner's data^{2,4} is, at most angles, their wide energy span from 5 to 30 MeV. Thus, it becomes possible to check the calculated results for energy-dependent weaknesses. Ideally, all excitation functions could be renormalized by means of the calculation. This could be very beneficial, in particular, in the cases of the five excitation functions at back angles depending on extrapolations. As Haesner's data were measured as excitation functions it comes natural to compare them with calculated excitation functions. Figs. 10 through 14 visualize this situation. Observe that the correction of Haesner's data² establishes the individual scales, too. Whereas the excitation function at 120 degrees has a perfect agreement in shape (0.4% rms. scatter of the measured data) and a quite reasonable agreement in scale (-3.0±1.2)% there is quite a mixed situation at the other angles. In particular, the systematic deviation at 150 degrees above about 12 MeV is quite disturbing. The situation is summed up in TABLE IV in numerical form. It appears that the calculation cannot provide a better normalization of the back-angle excitation functions, in particular at 150 and 160 degrees (Figs. 12 and 13).

TABLE IV. Numerical comparison of the five back-angle excitation functions.

Angle (lab. degrees)	Dev. from calc. scale %	rms. scatter of data points %
120	-3.0±1.2	0.4
135	1.5±1.1	1.1
150	5.3±1.0	2.4
160	3.3±1.2	2.0
178.8 ^{a)}	0.5±1.7	1.7

^{a)} shorter energy range

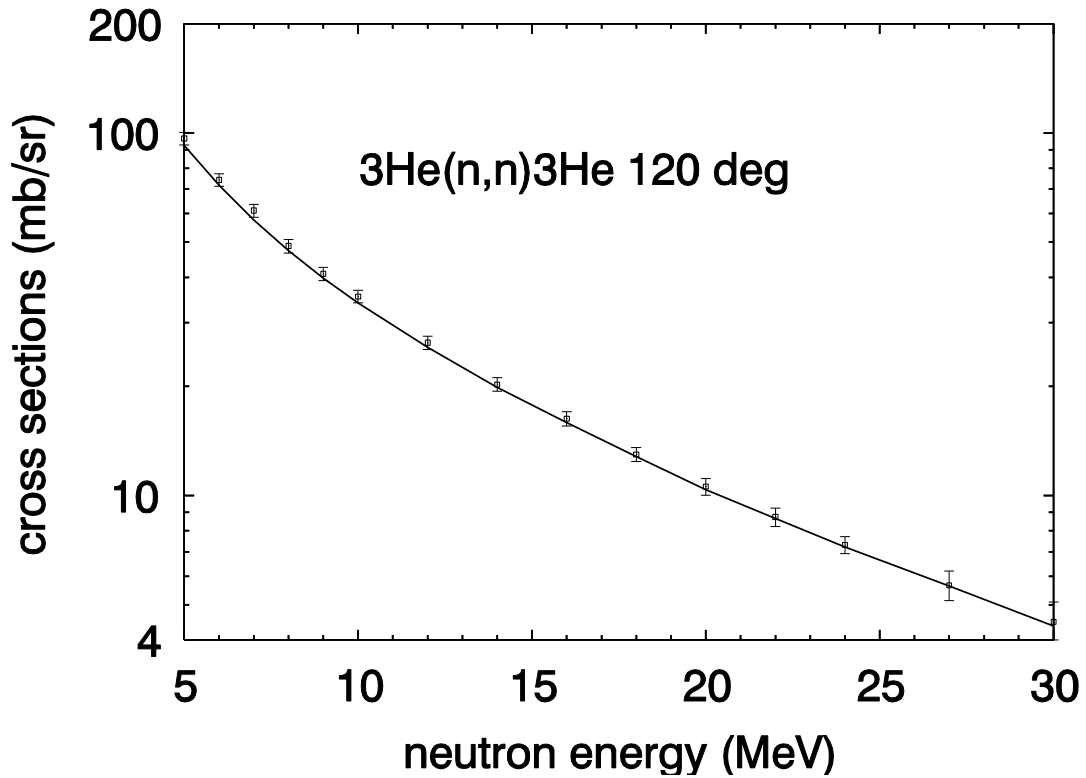


Fig. 10. Excitation function at 120 lab. degrees using c.m. cross sections. Haesner's corrected data^{2,4} vs. calculated values¹ (curve)

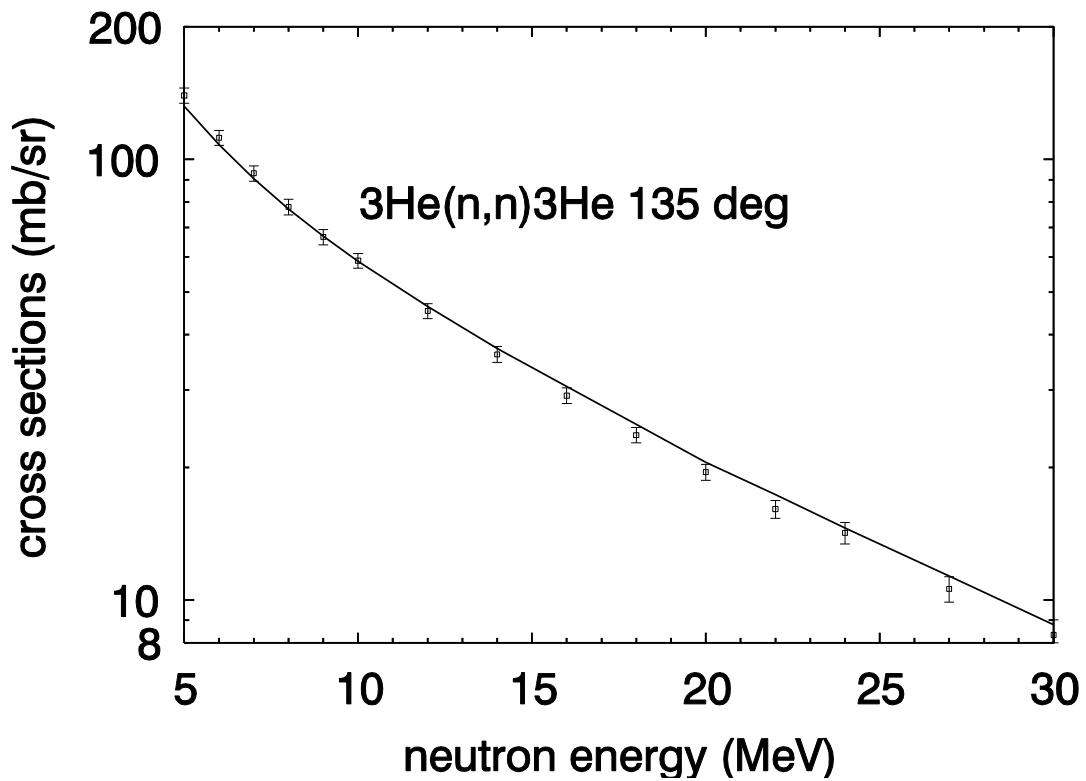


Fig. 11. Excitation function at 135 lab. degrees using c.m. cross sections. Haesner's corrected data^{2,4} vs. calculated values¹ (curve)

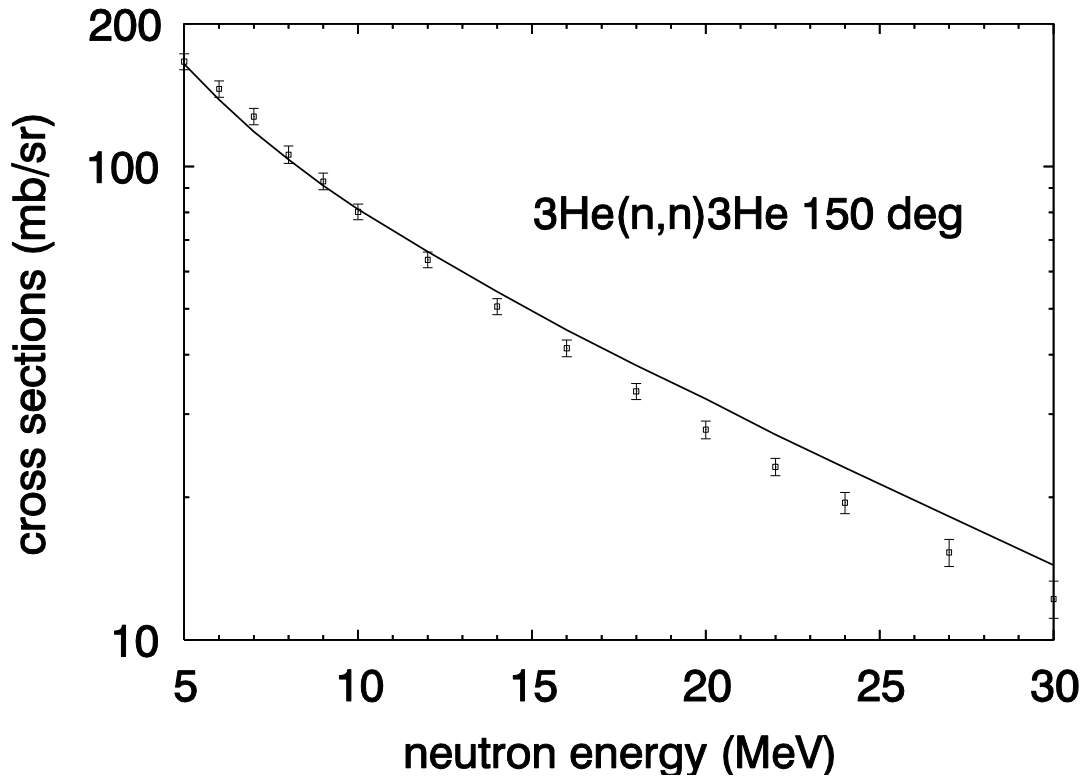


Fig. 12. Excitation function at 150 degrees. Haesner's corrected data^{2,4} vs. calculated values¹ (curve)

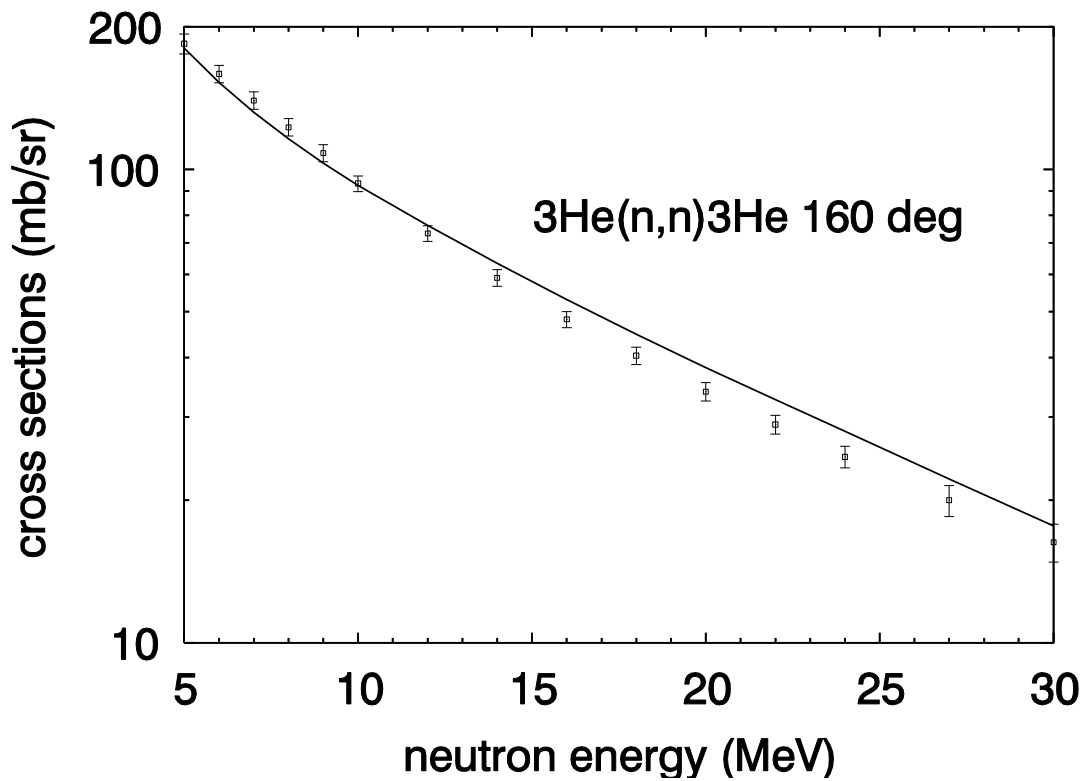


Fig. 13. Excitation function at 160 lab. degrees using c.m. cross sections. Haesner's corrected data^{2,4} vs. calculated values¹ (curve)

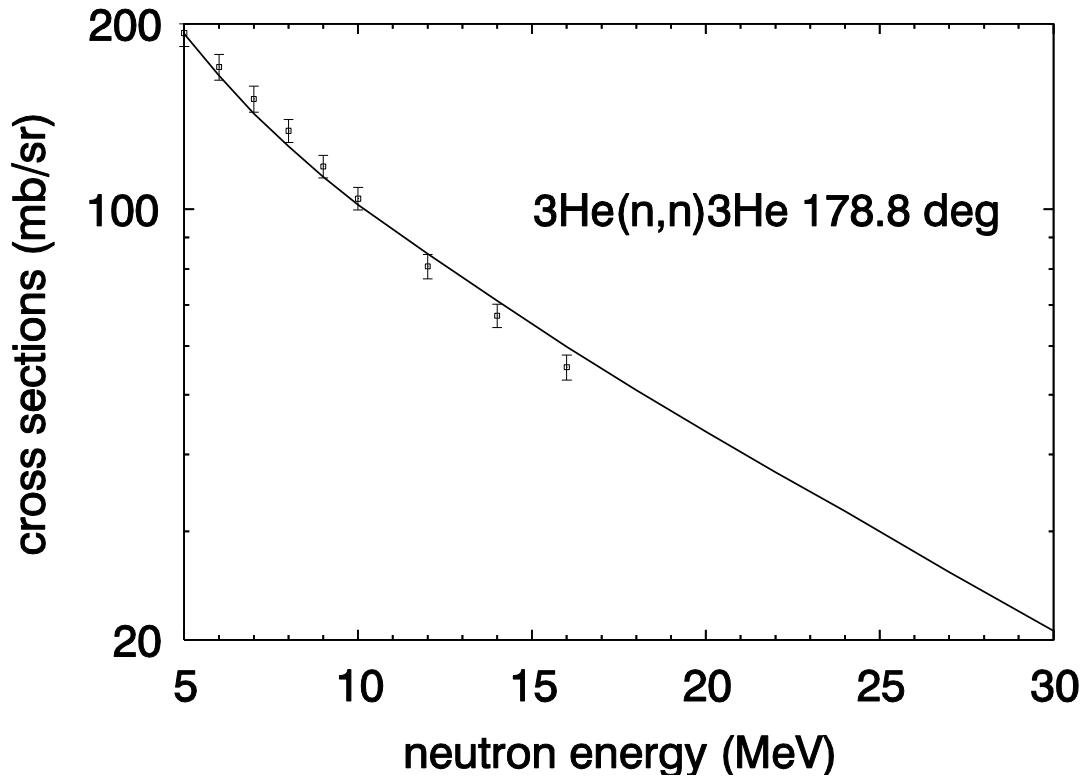


Fig. 14. Excitation function at 178.8 lab. degrees using c.m. cross sections. Haesner's corrected data^{2,4} vs. calculated values¹ (curve)

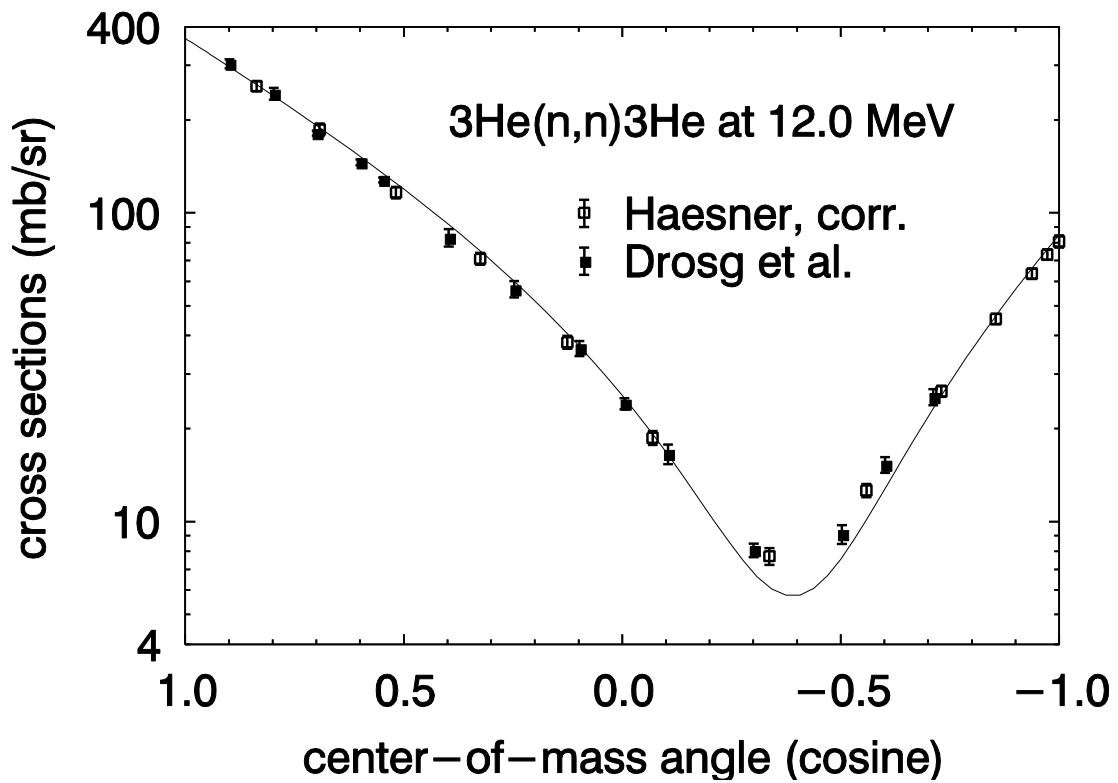


Fig. 15. Comparing the data at 12.0 MeV. The curve is calculated¹, the data points are experimental².

The greatest difference is obviously for the 150 degrees excitation function, in particular above 12 MeV. Up to about 12 MeV the agreement both in scale and shape is surprisingly good for all five excitation functions. This corroborates the evaluation work^{2,4} up to this energy, especially the new extrapolations from 135 degrees (c.m.) to 180 degrees. There is no obvious explanation for these substantial deviations of some excitation functions at higher energies.

To demonstrate the agreement at 12 MeV, Fig. 15 shows the solutions for the angle dependent differential cross sections. The agreement is excellent for both forward and backward angles, as is the case at 8 MeV (Fig. 4). Just the minima are deeper in the calculation which is not unexpected.

III. REEVALUATIONS

As discussed above, the absolute angle dependent differential cross sections of Drogg et al.² need to be up-scaled by a factor of 1.0367. As it is a constant factor for all data there is no need to do it individually. As these data form the backbone of the elastic cross section data, Table V recapitulates their main uncertainty contributions. From this table it becomes clear that a raise of the data by Drogg et al.^{2,4} (3.7±1.9)% is at the edge of being compatible with the magnitude of the total scale uncertainties in question as given in TABLE V (an excerpt of Table III of Ref. 2). However, the rms. scatter of 0.2% is highly compatible with the uncorrelated scale uncertainties given there.

TABLE V. Main scale uncertainty components of the reanalyzed LANL1974 data²

(A) Correlated Components (identical at all energies)					
(a) Connected with the standard:					
Accuracy of standard cross section	0.5%				
Mass of sample (abundance, weight)	0.5%				
Difference in subtended solid angle	1.1%				
(b) Connected with the sample:					
Mass (volume, purity, density)	1.0%				
Combined correlated uncertainties	1.7%				
(B) Uncorrelated Components (individual at each energy)					
	At primary energies of (MeV)				
	7.9	12.0	13.6	14.4	23.7
(a) Connected with the standard:					
Yield uncertainty (statistics, background)	2.2%	1.2%	2.4%	1.9%	2.1%
(b) Connected with the sample:					
Mass (density)	0.7%	0.6%	0.5%	0.7%	0.6%
Combined uncorrelated uncertainties	2.5%	1.4%	2.5%	2.2%	2.3%
(C) Total combined scale uncertainty	3.0%	2.2%	3.0%	2.7%	2.8%

TABLE VI. Re-normalized absolute differential center-of-mass cross sections derived from the corrected yield excitation functions of Haesner^{2,4}

E_n = 5.0 MeV			E_n = 6.0 MeV			E_n = 7.0 MeV		
θ_{cm} (°)	$d\sigma_{\text{cm}}/d\Omega$ (mb/sr)	$\Delta d\sigma/d\Omega$ (mb/sr)	θ_{cm}	$d\sigma_{\text{cm}}/d\Omega$	$\Delta d\sigma/d\Omega$	θ_{cm}	$d\sigma_{\text{cm}}/d\Omega$	$\Delta d\sigma/d\Omega$
33.16	399.	43.	33.17	381.	15.	33.17	351.	14.
46.10	-	-	46.11	309.	14.	46.12	271.	13.
58.73	259.	18.	58.74	217.9	9.6	58.75	189.8	8.5
70.96	164.9	8.4	70.97	155.2	7.7	70.98	140.4	6.6
82.71	77.9	6.0	82.72	74.9	5.2	82.73	67.8	4.1
93.91	50.0	2.7	93.92	40.6	2.3	93.93	33.5	2.0
109.60	42.8	3.2	109.61	27.3	2.0	109.62	19.2	1.5
123.90	60.8	3.9	123.91	39.7	2.3	123.92	32.4	1.8
136.88	96.6	3.9	136.89	74.2	3.0	136.90	61.1	2.5
148.71	139.63	5.7	148.72	112.0	4.4	148.73	93.0	3.7
159.65	166.4	6.6	159.65	145.8	5.8	159.66	127.5	5.0
166.58	184.2	8.9	166.59	159.0	6.8	166.59	139.7	5.9
179.20	193.2	9.3	179.20	170.2	8.2	179.20	151.1	7.4
E_n = 8.0 MeV			E_n = 9.0 MeV			E_n = 10.0 MeV		
θ_{cm}	$d\sigma_{\text{cm}}/d\Omega$	$\Delta d\sigma/d\Omega$	θ_{cm}	$d\sigma_{\text{cm}}/d\Omega$	$\Delta d\sigma/d\Omega$	θ_{cm}	$d\sigma_{\text{cm}}/d\Omega$	$\Delta d\sigma/d\Omega$
33.18	327.	13.	33.18	318.3	12.	33.19	298.8	11.
46.13	243.	12.	46.14	225.7	11.	46.15	212.1	9.5
58.76	167.0	7.5	58.77	151.8	6.4	58.78	137.8	5.7
70.99	122.5	5.7	71.00	110.5	4.9	71.01	94.9	4.2
82.74	57.8	3.2	82.75	51.2	2.5	82.76	46.6	2.1
93.95	29.1	1.7	93.96	25.7	1.5	93.97	23.0	1.2
109.63	15.5	1.2	109.64	12.5	0.83	109.65	10.7	0.63
123.93	24.6	1.4	123.94	21.0	1.2	123.95	18.3	0.92
136.90	48.8	2.1	136.91	42.4	1.7	136.92	36.7	1.4
148.73	78.0	3.2	148.74	69.1	2.7	148.74	61.1	2.3
159.66	105.9	4.5	159.67	98.0	3.7	159.67	84.5	3.1
166.59	122.7	5.2	166.59	111.4	4.5	166.60	96.1	3.6
179.20	134.1	5.8	179.20	120.6	5.0	179.20	107.0	4.4
E_n = 12.0 MeV			E_n = 14.0 MeV			E_n = 16.0 MeV		
θ_{cm}	$d\sigma_{\text{cm}}/d\Omega$	$\Delta d\sigma/d\Omega$	θ_{cm}	$d\sigma_{\text{cm}}/d\Omega$	$\Delta d\sigma/d\Omega$	θ_{cm}	$d\sigma_{\text{cm}}/d\Omega$	$\Delta d\sigma/d\Omega$
33.20	265.0	10.	33.22	233.6	9.0	33.23	233.4	9.0
46.16	193.0	8.6	46.18	162.6	6.6	46.20	144.3	6.0
58.80	120.6	5.02	58.82	105.1	4.3	58.84	90.1	3.7
71.04	73.6	3.2	71.06	61.6	2.7	71.08	50.3	2.2
82.79	39.5	1.8	82.81	29.6	1.4	82.83	23.6	1.1
93.99	19.4	0.99	94.02	-	-	94.04	12.5	0.60
109.67	8.01	0.49	109.70	6.35	0.37	109.72	4.65	0.26
123.97	13.1	0.63	123.99	9.16	0.46	124.01	7.11	0.33
136.94	27.4	1.1	136.95	21.0	0.86	136.97	16.9	0.73
148.76	47.0	1.8	148.77	37.5	1.5	148.78	30.2	1.2
159.68	66.9	2.4	159.69	53.3	2.0	159.69	43.5	1.7
166.60	75.4	2.8	166.61	60.6	2.4	166.61	49.6	1.9
179.20	83.1	3.7	179.20	69.0	2.9	179.20	56.9	2.6

E_n = 18.0 MeV			E_n = 20.0 MeV			E_n = 22.0 MeV		
θ_{cm}	$d\sigma_{\text{cm}}/d\Omega$	$\Delta d\sigma/d\Omega$	θ_{cm}	$d\sigma_{\text{cm}}/d\Omega$	$\Delta d\sigma/d\Omega$	θ_{cm}	$d\sigma_{\text{cm}}/d\Omega$	$\Delta d\sigma/d\Omega$
33.24	231.2	9.0	33.25	200.9	7.9	33.26	-	-
46.21	130.1	5.4	46.23	113.6	4.7	46.24	106.4	4.7
58.86	73.2	3.1	58.88	64.0	2.8	58.90	58.4	2.7
71.10	39.7	1.8	71.12	33.4	1.5	71.14	29.7	1.3
82.85	17.9	0.85	82.88	14.7	0.70	82.90	12.9	0.60
94.06	9.20	0.44	94.08	7.25	0.39	94.10	6.11	0.29
109.74	4.42	0.25	109.76	3.94	0.24	109.78	3.53	0.23
124.02	5.60	0.29	124.04	4.75	0.27	124.06	4.27	0.25
136.98	13.5	0.57	137.00	11.0	0.56	137.01	9.05	0.51
148.79	24.5	0.95	148.80	20.2	0.82	148.81	16.7	0.75
159.70	35.3	1.3	159.71	29.3	1.2	159.72	24.4	0.99
166.62	41.6	1.7	166.62	34.9	1.5	166.63	29.8	1.3
E_n = 24.0 MeV			E_n = 27.0 MeV			E_n = 30.0 MeV		
θ_{cm}	$d\sigma_{\text{cm}}/d\Omega$	$\Delta d\sigma/d\Omega$	θ_{cm}	$d\sigma_{\text{cm}}/d\Omega$	$\Delta d\sigma/d\Omega$	θ_{cm}	$d\sigma_{\text{cm}}/d\Omega$	$\Delta d\sigma/d\Omega$
46.26	99.0	4.5	46.29	84.5	4.2	46.31	67.7	3.9
58.92	52.1	2.6	58.95	44.6	2.3	58.98	37.8	2.2
71.16	27.8	1.3	71.20	24.9	1.3	71.23	19.6	1.0
82.92	12.3	0.7	82.96	11.7	0.7	82.99	9.53	0.63
94.13	5.47	0.27	94.16	4.91	0.27	94.19	4.58	0.36
109.80	3.23	0.21	109.84	2.87	0.20	109.87	2.68	0.21
124.08	3.98	0.24	124.11	3.72	0.32	124.14	3.40	0.31
137.03	7.58	0.47	137.05	5.87	0.53	137.08	4.65	0.60
148.83	14.8	0.8	148.84	11.0	0.7	148.86	8.64	0.72
159.72	20.5	1.0	159.74	16.1	1.0	159.75	12.9	1.1
166.63	25.5	1.3	166.64	20.6	1.5	166.65	17.0	1.5

Haesner's corrected excitation functions must be renormalized individually to fit into the up-scaled frame formed by the renormalized angular distribution data^{2,4}. These renormalized data are presented in Table VI by way of angle dependent differential cross sections.

From Legendre fits of the renormalized angle dependent differential cross sections elastic cross sections were derived (Table VII). Under the assumption that the two-body nonelastic cross sections are as accurate as stated unitary considerations now allow predictions of the three-body breakup cross sections. (Besides the impact of these cross sections on the following elaborations is rather small, as their share in the total cross section is small.)

The resulting breakup cross sections are fully compatible with the calculated values¹ (Table VIII). Observe that their uncertainties stem from the scale uncertainties of their components which are energy independent. Above agreement justifies an upscale by the full 3.7%, even if the conservative answer is just 2.0% (see Chapter V).

Fig. 16 shows the breakup cross sections of Table VII together with a curve based on the energy dependence of the calculated data¹.

TABLE VII. Energy dependence of revised (partial) cross sections of the n-³He interaction^{*)}

E_n	σ_T^a	σ_{el}^b	σ_{np}^c	σ_{nd}^d	σ_{bu}^e	$\Delta\sigma_{bu}$
3.5	2.785 ^f	2.248	0.537	0.000	0.	0.054
5.0	2.381 ^f	1.991	0.372	0.018	0.	0.047
6.0	2.145 ^f	1.797	0.305	0.043	0.	0.040
7.0	1.943 ^f	1.621	0.265	0.057	0.	0.038
7.9	1.796 ^f	1.490	0.236	0.065	0.005	0.034
8.0	1.779 ^f	1.470	0.233	0.065	0.011	0.033
9.0	1.637	1.342	0.215	0.071	0.009	0.031
10.0	1.513	1.236	0.196	0.074	0.007	0.029
12.0	1.317	1.060	0.165	0.076	0.016	0.024
13.6	1.197	0.943	0.145	0.075	0.034	0.022
14.0	1.158	0.911	0.140	0.075	0.032	0.022
14.4	1.130	0.890	0.136	0.074	0.030	0.021
16.0	1.039	0.805	0.121	0.072	0.041	0.019
18.0	0.946	0.712	0.105	0.068	0.061	0.017
20.0	0.863	0.640	0.092	0.064	0.067	0.015
22.0	0.791	0.568	0.082	0.059	0.082	0.014
23.7	0.738	0.520	0.074	0.056	0.088	0.013
24.0	0.732	0.517	0.0725	0.0552	0.087	0.013
27.0	0.652	0.4434	0.0604	0.0491	0.099	0.011
30.0	0.590	0.385	0.0506	0.0434	0.111	0.010

^{*)} Neutron energies are given in MeV, cross sections in barns

^a total cross sections from Refs. 2 and 4

^b elastic cross sections obtained from Legendre fits in the present analysis

^c nonelastic (n,p) cross sections from Refs. 3 and 4

^d nonelastic (n,d) cross sections from Refs. 3 and 4

^e many-body breakup cross sections from unitary considerations, or zero below the 7.33 MeV threshold

^f total cross sections from Ref. 6, divided by 1.0325, are up to 0.9% higher than those of Table I (column^b)

TABLE VIII. Numerical values of calculated (partial) cross sections¹ of the n-³He interaction^{*}

E_n	σ_T	σ_{el}	σ_{np}	σ_{nd}	σ_{bu}
3.5	2.654	2.140	0.515	0.000	0.000
5.0	2.295	1.909	0.366	0.021	0.000
5.5	2.179	1.812	0.333	0.035	0.000
6.0	2.085	1.730	0.310	0.044	0.000
7.0	1.902	1.573	0.272	0.058	0.000
8.0	1.745	1.437	0.242	0.064	0.002
10.0	1.493	1.219	0.198	0.071	0.005
12.0	1.302	1.048	0.166	0.073	0.016
14.4	1.125	0.886	0.137	0.070	0.032
16.0	1.029	0.800	0.122	0.067	0.042
17.1	0.974	0.748	0.114	0.064	0.049
22.0	0.780	0.566	0.085	0.053	0.077
23.7	0.726	0.516	0.078	0.049	0.083
27.0	0.645	0.439	0.066	0.042	0.098
30.0	0.585	0.385	0.058	0.035	0.106

^{*)} Neutron energies are given in MeV, cross sections in barns

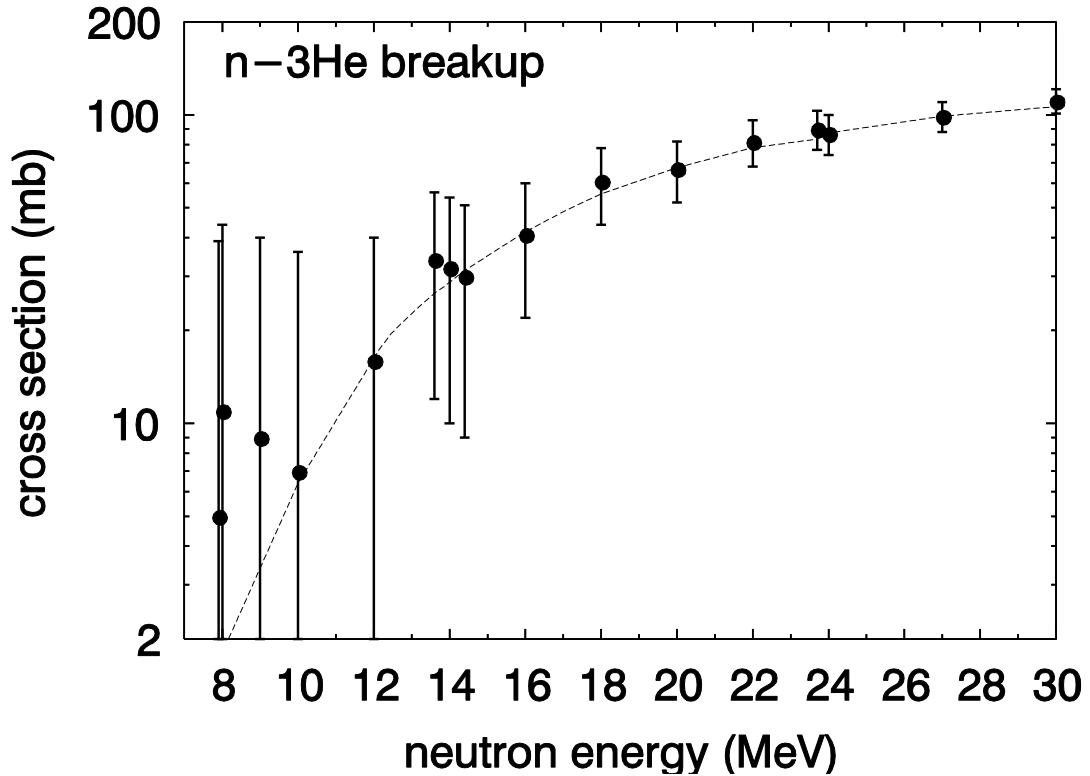


Fig. 16. n - ${}^3\text{He}$ breakup cross sections. The curve reflects the energy dependence of the calculated data¹

IV. DISCUSSION

It requires hard checking to find out how powerful the predictive force of a calculation is. Fortunately, there exists a consistent evaluation of n - ${}^3\text{He}$ cross sections in the energy range of interest^{2,4}. The main point of that evaluation, namely that the more recent total cross section data⁶ are high by more than 3% is wonderfully supported by the calculation which gives total cross sections which are even 4.5% lower. This is the main accomplishment. Above about 8 MeV the energy dependence of the total cross sections⁵ is perfectly supported by the calculation (Fig. 1).

Secondly, the front portion of all five data sets of differential cross sections between 7.9 and 23.7 MeV² are consistently 3.7% higher in the calculation. The experimental scale determination is governed by two components: the mass of the scattering sample, and by the normalization process.

The mass of the scattering sample is given by its volume and its density. Determining the effective volume is insofar tricky, as it involves the actual filling status of the sample container including its filling tube. This was investigated at some length and a combined 1.2% uncertainty was attributed to the mass. Repeating the measurement at three angles at 12 MeV

with a ^3He gas filling gave some insight in the correctness of the density values: The raw data show that the gas measurements gave (1.0186 ± 0.0187) higher values. This was taken as an agreement in scale. Now, it may be taken as too low a scale of the (liquid) measurements.

A difference of the effective volume from the nominal volume would not show up in this comparison. But there exists an in situ X-ray photograph of the filled cell. From it a 1.3% smaller volume can be deduced than from using the measures delivered by the workshop (contracted by the coolant). However, no confidence level is given for the X-ray value of that volume.

Considering the fact that, nominally, the two discussed effects in combination could have depressed the scale by 3.2% which is less than the required 3.7%, the remaining difference could be due to a problem in the normalization process. There, the main contributor to the uncertainty is the difference in subtended solid angle between standard sample and ^3He sample. A difference in the source-to-sample distance of only 0.08 cm would result in a 1.25% difference in subtended solid angle which is more than required. Considering the complicated construction of the liquid helium container (outer wall, heat shield, inner container) it is not unlikely that the effective position of the sample was not reproduced in the set-up of the cross section reference sample by better than 0.08 cm. Thus, independent of the actual cause, a 3.7% increase of the scale of the elastic data is not contradicted by experimental evidence. (Observe that the scale of the KARLSRUHE-1982 data depends on the LANL-1974 scale, i.e., the scales are 100% correlated.)

On the other hand, combining all scale information and assigning quite arbitrarily a 1.2% uncertainty to the calculated scale (i.e., the relative difference between the measured and the calculated scale of the total cross section) yields a scale factor of 1.020 ± 0.010 . However, taking the straight number 1.0367 as upscale factor of the measured elastic scattering data results in very reasonable breakup cross sections (Table VII). Besides, it is in the range, even if at the edge, of the experimental possibilities and considering the (correlated) scale uncertainty of 1.7% (Table V) it is statistically also in agreement with the 1.020 factor. However, it is likely to be an upper limit.

As there is no better way, the uncertainty discussion of Table V still applies to the present data, in spite of the shift in scale. After up-scaling all data based on the LANL-1974 experiment by 3.67% the angle dependent elastic differential cross sections between 5 and 14.4 MeV (Figs. 3, 6, 7, 9, and 15) are in very good agreement with the calculated data¹.

Measurements of differential elastic scattering cross sections in the minimum of the distribution are hampered by a strongly reduced signal-to-background ratio which is,

however, reflected in their higher uncertainties. Without further proof it would not be justified to disregard the experimental evidence. Thus, there is no pressing reason to change the shape of the elastic angle-dependent differential cross sections in the minimum.

The existence of (relative) excitation functions is particularly helpful in checking the energy dependence of the calculation. This check was only moderately successful. In particular, the calculated 150 and 160 degrees excitation functions of the elastic scattering differential cross sections are, beyond about 15 MeV, systematically higher than the experimental ones (Figs. 12, and 13). It is not clear whether the resulting stronger back-peaking of the calculated elastic differential cross sections at higher energies has sufficient substance to be considered even if $p\text{-}^3\text{He}$ and $p\text{-}^3\text{H}$ elastic scattering data exhibit a similar back-peaking at higher energies. The experimental evidence is very solid as it is based on an experiment using a source of white neutrons¹³. As, at each angle, data of all energies are obtained in a single measurement step, minimum problems in the determination of energy dependences of scattering data (differential excitation functions) are ensured.

ACKNOWLEDGEMENT

The invaluable support by Naohiko Otsuka of the Nuclear Data Section of IAEA is highly appreciated.

REFERENCES

- ¹A. Deltuva and A. C. Fonseca, “Calculation of neutron-He3 scattering up to 30 MeV”, Phys. Rev. C 90, 044002 (2014).
- ²M. Drosig, R. Avalos Ortiz, and P. W. Lisowski: “Neutron interactions with ^3He revisited I. Elastic scattering around and beyond 10 MeV”, Nucl. Sci. Eng. 172, 87 (2012).
- ³M. Drosig, P. W. Lisowski: “Neutron interactions with ^3He revisited II. Nonelastic cross sections in the Mega-electron-volt range”, Nucl. Sci. Eng. 175, 19 (2013).
- ⁴M. Drosig, “Neutron interactions with ^3He revisited III. Neutron cross sections between 24 and 30 MeV”, Nucl. Sci. Eng. 180, 341 (2015).
- ⁵ C. A. Goulding, P. Stoler, and J. D. Seagrave, “ ^3He and ^4He total neutron cross sections in the MeV region”, Nucl. Phys. A, 215, 253 (1973).
- ⁶ B. Haesner, W. Heeringa, H. O. Klages, H. Dobiash, G. Schmalz, P. Schwarz, J. Wilczynski, and B. Zeitnitz, “Measurement of the ^3He and ^4He total neutron cross sections up

to 40 MeV”, *Phys. Rev. C*, 28, 995 (1983).

⁷A. I. Abramov, *Zh. Exp. Teor. Fiz.*, 37, 1476 (1959) [translation in *Sov. Phys. JETP*, 10, 1046 (1960)].

⁸A. R. Sayres, K. W. Jones, and C. S. Wu, “Interaction of neutrons with ^3He ”, *Phys. Rev.*, 122, 1853 (1961).

⁹B. Antolkovic, M. Cerineo, G. Paic, P. Tomas, V. Ajdacic, B. Lalovic, W. T. H. Van Oers, and I. Slaus, “A study of the neutron- ^3He interaction at 14.4 MeV”, *Phys. Lett.*, 23, 477 (1966).

¹⁰B. Antolkovic, G. Paic, P. Tomas, and D. Rendic, “Study of neutron-induced reactions on ^3He at $E_n=14.4$ MeV”, *Phys. Rev.*, 159, 777 (1967).

¹¹R. H. Curtis, “Elastic scattering of 14-MeV neutrons from He-3”, *Dissertation Abstracts B (Sciences)*, 33, 3866 (1973).

¹²J. D. Seagrave, L. Cranberg, and J. E. Simmons, “Elastic scattering of fast neutrons by tritium and ^3He ”, *Phys. Rev.*, 119, 1981 (1960).

¹³B. Haesner, Master Thesis, “Experimente zur Bestimmung der Wirkungsquerschnitte für das n- ^3He -System im Energiebereich von 1 bis 40 MeV”, Report KfK-3395, Kernforschungszentrum Karlsruhe, Aug. 1982.

¹⁴W. Glöckle, H. Witała, D. Hüber, H. Kamada, and J. Golak, “The three-nucleon continuum: achievements, challenges and applications”, *Phys. Rep.* 274, 107 (1996)

A. Kievsky, M. Viviani, and S. Rosati, “Polarization observables in p-d scattering below 30 MeV”, *Phys. Rev. C* 64, 024002 (2001).

A. Deltuva, A. C. Fonseca, and P. U. Sauer, “Momentum-space treatment of Coulomb interaction in three-nucleon reactions with two protons”, *Phys. Rev. C* 71, 054005 (2005).

¹⁵A. Deltuva, and A. C. Fonseca, “Calculation of proton- ^3He elastic scattering between 7 and 35 MeV”, *Phys. Rev. C* 87, 054002 (2013).

Nuclear Data Section
International Atomic Energy Agency
P.O. Box 100
A-1400 Vienna
Austria

e-mail: nds.contact-point@iaea.org
fax: (43-1) 26007
telephone: (43-1) 2600 21725
Web: <http://www-nds.iaea.org/>